COMPLIANT MOTION CONTROLLERS FOR KINEMATICALLY REDUNDANT MANIPULATORS

Jonghoon Park*, Wan-Kyun Chung**, Youngil Youm**

* Graduate Student in Dept. of Mech. Eng, Pohang University of Science and Technology (POSTECH)
** Professors in Dept. of Mech. Eng, Pohang University of Science and Technology (POSTECH)
Tel:+82-562-279-2844; Fax: +82-562-279-5899; E-mail: jhpark@risbot.rist.re.kr

Abstracts The problem of compliant motion control using a redundant manipulator is addressed in this article. Specifically, a hybrid-control type and impedance-control type controllers are extended to general redundant manipulators based on the kinematically decomposed and geometrically compatible modeling of its joint space. In the case of the hybrid controller, it leads to the linear and decoupled closed-loop dynamics in the three motion spaces, that is the motion-controlled, force-controlled, and the null motion-controlled spaces of the redundant manipulator. When the proposed impedance controller is applied, the decoupled impedance models in three motion spaces are obtained. The superiority of the proposed controllers is verified with the numerical experiments.

Keywords Kinematic redundancy, Kinematically decomposed and geometrically compatible modeling, Compliant motion controller

INTRODUCTION

To apply a manipulator into a task in presence of contact with environments, a compliant motion controller is required. The design of a compliant motion controller was complicated when the manipulator is kinematically redundant [1, 6, 7]. The main obstruction is involvement of possible null motions, which are intrinsic in redundant manipulators. Recently, a dynamic controller, called the kinematically decomposed dynamic controller, was proposed for redundant manipulators which can guarantee stable null motion dynamics [8].

This article attempts to incorporate the conventional compliant motion controllers, that is the hybrid position/force controller [3, 5, 9] and the impedance controller [4], into the kinematically decomposed dynamic controller. First, the equations of motion of redundant manipulators are reformulated to ones oriented to the compliant motion controller design, based on the kinematically decomposed and geometrically compatible modeling. Next, we propose two compliant motion controllers for redundant manipulators.

KINEMATIC DECOMPOSITION OF THE JOINT SPACE

Assume that the pose of a manipulator is denoted by a joint configuration $\boldsymbol{q} \in \Re^n$ and a task space is parametrized with m independent coordinates. The degrees of redundancy is $r = n - m$. Recently, a useful coordinate transformation was proposed [8], called the kinematically decomposed modeling, under which a joint velocity $\dot{\boldsymbol{q}}$ can be decomposed into

$$\dot{\boldsymbol{q}} = \boldsymbol{R}(\boldsymbol{q})\dot{\boldsymbol{q}}_{net} + \boldsymbol{N}(\boldsymbol{q})\dot{\boldsymbol{q}}_{null}. \tag{1}$$

The matrices $\boldsymbol{R} \in \Re^{n\times m}$ and $\boldsymbol{N} \in \Re^{n\times r}$ are submatrices of the right singular matrix of the manipulator Jacobian $\boldsymbol{J} \in \Re^{m\times n}$, that is

$$\boldsymbol{J} = \boldsymbol{U}\,[\;\boldsymbol{\Sigma}\quad 0\;]\,[\;\boldsymbol{R}\quad \boldsymbol{N}\;]^T, \tag{2}$$

where $\boldsymbol{U} \in \Re^{m\times m}$ is the orthogonal matrix, and $\boldsymbol{\Sigma} \in \Re^{m\times m}$ is a diagonal matrix of the singular values of $\boldsymbol{J}$.

The matrices $\boldsymbol{R}$ and $\boldsymbol{N}$ enables the following three properties: the minimal representation property,

$$\dot{\boldsymbol{q}}_p \triangleq \boldsymbol{J}^+\boldsymbol{J}\dot{\boldsymbol{q}} = \boldsymbol{R}\dot{\boldsymbol{q}}_{net} \tag{3}$$

$$\dot{\boldsymbol{q}}_h \triangleq (\boldsymbol{I} - \boldsymbol{J}^+\boldsymbol{J})\dot{\boldsymbol{q}} = \boldsymbol{N}\dot{\boldsymbol{q}}_{null} \tag{4}$$

the filtering property,

$$\dot{\boldsymbol{q}}_{net} = \boldsymbol{R}^T\dot{\boldsymbol{q}} \tag{5}$$

$$\dot{\boldsymbol{q}}_{null} = \boldsymbol{N}^T\dot{\boldsymbol{q}} \tag{6}$$

and the correspondence with the task velocity,

$$\dot{\boldsymbol{q}}_{net} = (\boldsymbol{J}\boldsymbol{R})^{-1}\dot{\boldsymbol{p}}. \tag{7}$$

Rearranging Eqs. (3) and (4) in matrix form, we get a coordinate transformation as following:

$$\dot{\boldsymbol{q}} = \boldsymbol{R}(\boldsymbol{J}\boldsymbol{R})^{-1}\dot{\boldsymbol{p}} + \boldsymbol{N}\dot{\boldsymbol{q}}_{null} \tag{8}$$

Using the above coordinate transformation matrix, the joint acceleration is expressed by

$$\ddot{\boldsymbol{q}} = \boldsymbol{R}\ddot{\boldsymbol{q}}_{net} + \boldsymbol{N}\ddot{\boldsymbol{q}}_{null} + \dot{\boldsymbol{R}}\dot{\boldsymbol{q}}_{net} + \dot{\boldsymbol{N}}\dot{\boldsymbol{q}}_{null}. \tag{9}$$

The calculations of $\dot{\boldsymbol{R}}$ and $\dot{\boldsymbol{N}}$ are required and was analytically found in [8].

GEOMETRICALLY COMPATIBLE TASK SPACE DECOMPOSITION

Let us introduce an additional coordinate transformation which transforms the standard coordinates of the task space into new orthogonal ones. The new orthogonal coordinates can be same as the standard ones, or can be new ones which are useful to describe some compliant motion task. We are to define new coordinate value vectors, denoted by $\dot{\boldsymbol{r}}_F \in \Re^k$ and $\dot{\boldsymbol{r}}_P \in \Re^l (l = m - k)$, with suitable coordinate bases $\boldsymbol{E}_F \in \Re^{m\times k}$ and $\boldsymbol{E}_P \in \Re^{m\times l}$, and decompose $\dot{\boldsymbol{p}} \in \Re^m$ as follows

$$\dot{\boldsymbol{p}} = [\;\boldsymbol{E}_P\quad \boldsymbol{E}_F\;]\begin{pmatrix} \dot{\boldsymbol{r}}_P \\ \dot{\boldsymbol{r}}_F \end{pmatrix}. \tag{10}$$

The compatible coordinates to a given task geometry which is specified with the equations of hypersurface (on which the task is to be executed in usual applications)

$$0 = \boldsymbol{\phi}(\boldsymbol{p}) = \begin{pmatrix} \phi_1(\boldsymbol{p}) \\ \vdots \\ \phi_k(\boldsymbol{p}) \end{pmatrix} \tag{11}$$

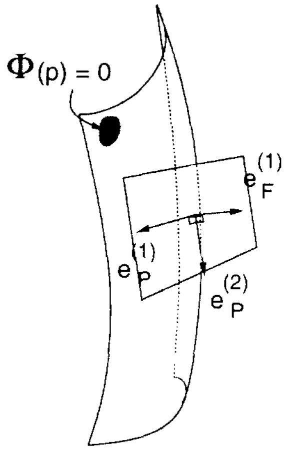

Figure 1. Task description in 3 dimensional space

is obtained as follows. Let us denote by $\boldsymbol{J}_\phi$ the Jacobian of $\boldsymbol{\phi}(\boldsymbol{p})$. The singular value decomposition of $\boldsymbol{J}_\phi \in \Re^{k\times m}$ yields the right singular matrix $\boldsymbol{V}_\phi$

$$\boldsymbol{V}_\phi = [\ \boldsymbol{E}_F \quad \boldsymbol{E}_P\ ], \tag{12}$$

where $\boldsymbol{E}_F \in \Re^{m\times k}$ and $\boldsymbol{E}_P \in \Re^{m\times l}$. By Defining $\dot{\boldsymbol{r}}_P$ and $\dot{\boldsymbol{r}}_F$ as

$$\dot{\boldsymbol{r}}_P = \boldsymbol{E}_P^T\dot{\boldsymbol{p}} \tag{13}$$
$$\dot{\boldsymbol{r}}_F = \boldsymbol{E}_F^T\dot{\boldsymbol{p}}, \tag{14}$$

we obtain the geometrically compatible task space decomposition. The matrices $\boldsymbol{E}_P$ and $\boldsymbol{E}_F$ can be calculated in a similar way as $\boldsymbol{R}$ and $\boldsymbol{N}$.

For example, if we are given one equation which defines a constraint, say $\phi(\boldsymbol{p}) = 0$, then it defines the surface in 3 dimensional task space. Then taking the right singular matrix of $\boldsymbol{J}_\phi \in \Re^{1\times 3}$ we get $\boldsymbol{E}_P = [\boldsymbol{e}_P^{(1)}|\boldsymbol{e}_P^{(2)}]$ and $\boldsymbol{E}_F = [\boldsymbol{e}_F^{(1)}]$. They can be geometrically visualized as Fig. 1.

FORMULATION OF EQUATIONS OF MOTION

Taking the transformations Eq. (10) with Eq. (8), we get the following unique transformation matrix

$$\left[\boldsymbol{R}(\boldsymbol{JR})^{-1}|\boldsymbol{N}\right]\begin{bmatrix}[\boldsymbol{E}_P|\boldsymbol{E}_F] & 0\\ 0 & \boldsymbol{I}\end{bmatrix}\begin{pmatrix}\dot{\boldsymbol{r}}_P\\ \dot{\boldsymbol{r}}_F\\ \dot{\boldsymbol{q}}_{null}\end{pmatrix} = \dot{\boldsymbol{q}}. \tag{15}$$

Hereafter, we call this equation the *kinematically decomposed and geometrically compatible modeling*, since a joint variable $\dot{\boldsymbol{q}}$ is decomposed into the null motion variable and the task variable which again is decomposed into two subspaces which are compatible to a given task geometry. By the duality between the motion and force at the static equilibrium, the torque $\boldsymbol{\tau} \in \Re^n$ and each force denoted by $\boldsymbol{f}_P \in \Re^l$, $\boldsymbol{f}_F \in \Re^k$, or $\boldsymbol{\tau}_{null} \in \Re^r$ respectively, which defines a work with each decomposed motion variable (or $\dot{\boldsymbol{r}}_P$, $\dot{\boldsymbol{r}}_F$, $\dot{\boldsymbol{q}}_{null}$), are related by

$$\boldsymbol{\tau} = \boldsymbol{J}^T\{\boldsymbol{E}_P\boldsymbol{f}_P + \boldsymbol{E}_F\boldsymbol{f}_F\} + \boldsymbol{N}\boldsymbol{\tau}_{null}. \tag{16}$$

In the mean time, let us assume that the dynamic equations of a redundant manipulator are of the form

$$\boldsymbol{\tau} = \boldsymbol{M}(\boldsymbol{q})\ddot{\boldsymbol{q}} + \boldsymbol{h}(\boldsymbol{q},\dot{\boldsymbol{q}}), \tag{17}$$

where $\boldsymbol{M}(\boldsymbol{q}) \in \Re^{n\times n}$ is the inertia matrix and $\boldsymbol{h}(\boldsymbol{q},\dot{\boldsymbol{q}}) \in \Re^n$ denotes all the dynamic forces except the inertial torque. Expressing the equations of motion in Eq. (17) with respect to the new coordinates yields a different, but equivalent, equations of motion

$$\begin{aligned}\boldsymbol{\tau} &= \boldsymbol{M}\left[\boldsymbol{R}(\boldsymbol{JR})^{-1}|\boldsymbol{N}\right]\begin{bmatrix}[\boldsymbol{E}_P|\boldsymbol{E}_F] & 0\\ 0 & \boldsymbol{I}\end{bmatrix}\begin{pmatrix}\ddot{\boldsymbol{r}}_P\\ \ddot{\boldsymbol{r}}_F\\ \ddot{\boldsymbol{q}}_{null}\end{pmatrix}\\ &+ \boldsymbol{M}\frac{\mathrm{d}}{\mathrm{d}t}\left[\boldsymbol{R}(\boldsymbol{JR})^{-1}|\boldsymbol{N}\right]\begin{bmatrix}[\boldsymbol{E}_P|\boldsymbol{E}_F] & 0\\ 0 & \boldsymbol{I}\end{bmatrix}\begin{pmatrix}\dot{\boldsymbol{r}}_P\\ \dot{\boldsymbol{r}}_F\\ \dot{\boldsymbol{q}}_{null}\end{pmatrix}\\ &+ \boldsymbol{M}\boldsymbol{R}(\boldsymbol{JR})^{-1}\frac{\mathrm{d}}{\mathrm{d}t}[\boldsymbol{E}_P|\boldsymbol{E}_F]\begin{pmatrix}\dot{\boldsymbol{r}}_P\\ \dot{\boldsymbol{r}}_F\end{pmatrix}\\ &+ \boldsymbol{h} + \boldsymbol{J}^T\{\boldsymbol{E}_P\boldsymbol{f}_P + \boldsymbol{E}_F\boldsymbol{f}_F\} + \boldsymbol{N}\boldsymbol{\tau}_{null}.\end{aligned} \tag{18}$$

The equations of motion is called the *kinematically decomposed and geometrically compatible dynamic equations* of redundant manipulators.

IN HYBRID CONTROL FASHION

Hybrid position/force controller [3, 5, 9] attempts to directly utilize the information on the task geometry. The hybrid controller is valid on the assumptions, referred to as the orthogonality of the motion-controlled and force-controlled subspaces, and the assumptions are expressed in our formulation as

$$0 = \dot{\boldsymbol{r}}_F = \ddot{\boldsymbol{r}}_F \tag{19}$$
$$0 = \boldsymbol{f}_P. \tag{20}$$

When there is assumed to exist no constraints in self-motion of manipulators, it is

$$\boldsymbol{\tau}_{null} = 0. \tag{21}$$

On the belief that the assumptions are valid, we design a dynamic hybrid controller using the kinematically decomposed and geometrically compatible dynamic model of redundant manipulators. First, we define a feedback linearization law, to compensate all nonlinearities involved in robot motion, as follows

$$\begin{aligned}\boldsymbol{\tau} &= \boldsymbol{M}\left[\boldsymbol{R}(\boldsymbol{JR})^{-1}|\boldsymbol{N}\right]\begin{bmatrix}[\boldsymbol{E}_P|\boldsymbol{E}_F] & 0\\ 0 & \boldsymbol{I}\end{bmatrix}\begin{pmatrix}\boldsymbol{u}_P\\ 0\\ \boldsymbol{u}_{null}\end{pmatrix}\\ &+ \boldsymbol{J}^T\boldsymbol{E}_F\boldsymbol{u}_F + \tilde{\boldsymbol{h}}\end{aligned} \tag{22}$$

where $\tilde{\boldsymbol{h}}(\boldsymbol{q},\dot{\boldsymbol{q}})$ is

$$\begin{aligned}\tilde{\boldsymbol{h}} &= \boldsymbol{M}\frac{\mathrm{d}}{\mathrm{d}t}\left[\boldsymbol{R}(\boldsymbol{JR})^{-1}|\boldsymbol{N}\right]\begin{bmatrix}[\boldsymbol{E}_P|\boldsymbol{E}_F] & 0\\ 0 & \boldsymbol{I}\end{bmatrix}\begin{pmatrix}\dot{\boldsymbol{r}}_P\\ \dot{\boldsymbol{r}}_F\\ \dot{\boldsymbol{q}}_{null}\end{pmatrix}\\ &+ \boldsymbol{M}\boldsymbol{R}(\boldsymbol{JR})^{-1}\left[\dot{\boldsymbol{E}}_P|\dot{\boldsymbol{E}}_F\right]\begin{pmatrix}\dot{\boldsymbol{r}}_P\\ \dot{\boldsymbol{r}}_F\end{pmatrix} + \boldsymbol{h}.\end{aligned} \tag{23}$$

Second, it remains to design a outer loop controller to stabilize the feedback-linearized closed loop system.

If the assumptions of Eqs. (21), (19), and (20) are valid, then the closed loop systems are decomposed into three spaces, and each is linearized:

$$0 = \boldsymbol{u}_P - \ddot{\boldsymbol{r}}_P \tag{24}$$
$$0 = \boldsymbol{u}_F - \boldsymbol{f}_F \tag{25}$$
$$0 = \boldsymbol{u}_{null} - \ddot{\boldsymbol{q}}_{null}, \tag{26}$$

Table 1. Parameters of the manipulator

	length $l(m)$	c.o.m. $r(m)$	mass $m(kg)$	inertia $I(kg \times m^2)$
1	0.3	0.15	20.0	0.15
2	0.25	0.125	10.0	0.0521
3	0.2	0.1	10.0	0.0333

if the following matrix is nonsingular

$$\tilde{A}(q) = [\ MR(JR)^{-1}E_P \quad J^T E_F \quad MN\ ]. \quad (27)$$

IN IMPEDANCE CONTROL FASHION

In this section we develop an impedance controller [2, 4] based on the kinematically decomposed and geometrically compatible dynamic model of redundant manipulators. We want to reshape the dynamics of manipulator to have the following decoupled target impedances

$$\begin{aligned} f_P &= M_P\ddot{e}_P + D_P\dot{e}_P + K_P e_P & (28)\\ f_F &= M_F\ddot{e}_F + D_F\dot{e}_F + K_F e_F & (29)\\ \tau_{null} &= D_n\ddot{e}_{null} + K_n\dot{e}_{null}, & (30)\end{aligned}$$

where $e_P = r_{P,d} - r_P$, $e_F = r_{F,d} - r_F$, and $\dot{e}_{null} = \dot{q}_{null,d} - \dot{q}_{null}$.

To achieve the target impedances, the following control law should be used

$$\begin{aligned}\tau &= \tilde{h} \quad (31)\\ &+ M\left[R(JR)^{-1}|N\right]\begin{bmatrix}[E_P|E_F] & 0\\ 0 & I\end{bmatrix}\\ &\times\begin{pmatrix}\ddot{r}_{P,d} + M_P^{-1}(D_P\dot{e}_P + K_P e_P)\\ \ddot{r}_{F,d} + M_F^{-1}(D_F\dot{e}_F + K_F e_F)\\ \ddot{q}_{null,d} + D_n^{-1}K_n\dot{e}_{null}\end{pmatrix}\\ &+ \left\{-M\left[R(JR)^{-1}|N\right]\begin{bmatrix}[E_P|E_F] & 0\\ 0 & I\end{bmatrix}\Lambda^{-1}\right.\\ &\left.+ [\ J^T E_P \quad J^T E_F \quad N\ ]\right\}\begin{pmatrix}f_P\\ f_F\\ \tau_{null}\end{pmatrix}, \quad (32)\end{aligned}$$

where

$$\Lambda^{-1}(q) = \begin{bmatrix} M_P^{-1} & 0 & 0\\ 0 & M_F^{-1} & 0\\ 0 & 0 & D_n^{-1}\end{bmatrix}. \quad (33)$$

Note that the null motion is modulated by the null motion impedance, which guarantees the stable zero dynamics of the redundant manipulator.

NUMERICAL EXPERIMENTS

A planar 3-dof manipulator is employed to simulate the controllers. The parameters are shown in Table 1.

There is assumed to exist a frictionless vertical wall at $x = 0.4(m)$, whose right-hand side is constrained. The constrained force is modeled as the spring and damping force, whose stiffness and damping coefficients are: $K_{env} = 100000(N/m)$, and $D_{env} = 100(N \cdot sec/m)$. That is,

$$f_{env} = K_{env}(x - 0.4) + D_{env}\dot{x}. \quad (34)$$

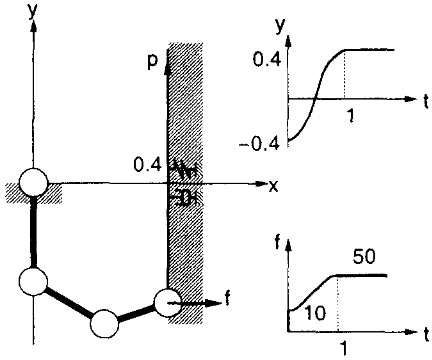

Figure 2. Description of the simulated system

The desired trajectory is the straight line from $(0.4, -0.4)(m)$ to $(0.4, 0.4)(m)$ which is interpolated, during $1(sec)$ by the quintic polynomial with zero velocity and jerk condition at the boundaries. The desired forces at the initial and final position are $(10, 0)(N)$ and $(50, 0)(N)$. The intermediate force trajectory is generated by the linear parabolic blend interpolation. The desired null motion was generated in order to maximize the manipulability measure $m(q)$ as following [8]

$$\dot{q}_{null,d} = \kappa N^T \nabla m, \quad (35)$$

where $\kappa = 100$.

The initial state of the manipulator is: $q_0 = (-90.0, 54.9928, 47.5458)(°)$, $\dot{q}_0 = (0.0, 0.0, 0.0)\ (rad/sec)$, and the initial torque is set zero. Note that the initial configuration corresponds to the initial position, while the desired initial force $10N$ cannot be achieved at the initial configuration. That is, at $t = 0.0$ the force trajectory is a kind of step input. Thereafter it is linear-parabolically blended ramp input. The description of the simulated system is illustrated in Fig. 2.

The controller is implemented on the assumption that the state of the manipulator $(q^T, \dot{q}^T)^T$ and the tip force f are perfectly measured and the parameter is exactly estimated. Also, there is assumed to be no hardware limitations, for example, in achievable torque and joint travel limit. The control frequency is set by $1kHz$. As the servo outer loops for the hybrid position/force control, we employ the following simple linear controllers:

$$\begin{aligned} u_P &= \ddot{r}_{P,d} + K_P e_P + D_P\dot{e}_P + I_P\int e_P & (36)\\ u_F &= f_{F,d} + K_F\epsilon_F + I_F\int\epsilon_F & (37)\\ u_{null} &= \ddot{q}_{null,d} + K_n\dot{e}_{null} + I_n\int\dot{e}_{null}, & (38)\end{aligned}$$

where $\epsilon_F = f_{F,d} - f_F$, $e_P = r_{P,d} - r_P$, and $\dot{e}_{null} = \dot{q}_{null,d} - \dot{q}_{null}$. When the gains are: $K_p = 1000$, $D_P = 50$, $I_P = 5$, $K_F = 10$, $I_F = 10$, $K_n = 100$, $I_n = 0$, the control performance is shown in Fig. 3.

For the impedance controller configuration, the desired decomposed impedance parameters are set as: $K_P = 1000$, $D_P = 22$, $M_P = 1$, $K_F = 1000$, $D_F = 100$, $M_F = 5$, $K_n = 100$, $D_n = 1$. The simulation result is shown in Fig. 4. Note that the desired x-trajectory was modified to generate the similar force trajectory as seen in Fig. 4 (d). That is, the virtual x-trajectory is from $0.41(m)$ to $0.46(m)$.

In both cases, the expected control performance was achieved. The initial oscillations in torque and joint velocity are due to the step response of force trajectory. Note that the force as well as null velocity responses show exponentially tracking property in spite of the initial error. Also, the tracking performance in the motion-controlled space is not affected by the initial errors in force and null motion.

CONCLUSION

In this article the compliant motion controllers for kinematically redundant manipulators were developed. They are based on the kinematically decomposed and geometrically compatible modeling of joint space. The modeling is general and analytic. The main advantage of the proposed controllers is that they can decompose the closed-loop dynamics of the manipulator into the motion-controlled, force-controlled, and null motion-controlled spaces, and reshape each into linear and decoupled one.

References

[1] Peng, Z.-X., and N. Adachi, "Compliant motion control of kinematically redundant manipulators", in *IEEE. Trans. on Robotics and Automation*, vol. 9, no. 6, pp. 831–837, 1993

[2] Anderson, R. J., and M. W. Spong, "Hybrid Impedance control of robot manipulators", in *IEEE. J. of Robotics and Automation*, vol. 4, no. 5, pp. 549–556, 1988

[3] Raibert, M. H., and J. J. Craig, "Hybrid position/force control of manipulators", in *Tran. ASME J. of Dynamic Systems, Measurement, and Control*, vol. 102, no. 3, pp. 126–133, 1981

[4] Hogan, N., "Impedance control: An approach to manipulation: Part I, II, III", in *Tran. ASME J. of Dynamic Systems, Measurement, and Control*, vol. 107, no. 3, pp. 1–24, 1985

[5] Khatib, O., "A unified approach for motion and force control of robot manipulators: The operational space formulation", in *IEEE J. of Robotics and Automation*, vol. RA-3, no. 1, pp. 43–53, 1987

[6] Lozano, R., and B. Brogliato, "Adaptive hybrid force-position control for redundant manipulators" in *IEEE. Trans. on Automatic Control*, vol. 37, no. 10, pp. 1501–1505, 1992

[7] Newman, W. S., and M. E. Dohring, "Augmented impedance control: An approach to compliant motion control of kinematically redundant manipulators", in *Proc. 1991 IEEE Int. Conf. on Robotics and Automation*, pp. 30–35, 1991

[8] Park, J., W.-K. Chung, and Y. Youm, "Specification and control of motion for kinematically redundant manipulators", in *Proc. 1995 IEEE/RSJ Int. Conf. on Intelligent Robots and Systems*, vol. 3, pp. 89–94, 1995

[9] Yoshikawa, T., "Dynamic hybrid position/force control of robot manipulators-Description of hand constraints and joint driving force", in *IEEE J. of Robotics and Automation*, vol. RA-3, no. 5, pp. 386–392, Oct. 1987

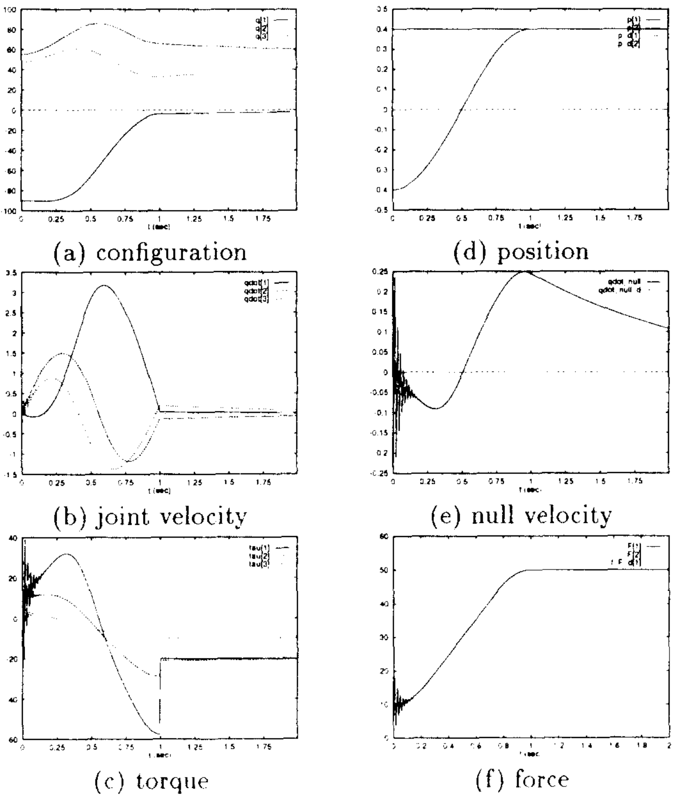

(a) configuration (d) position (b) joint velocity (e) null velocity (c) torque (f) force

Figure 3. Simulation result in hybrid control fashion

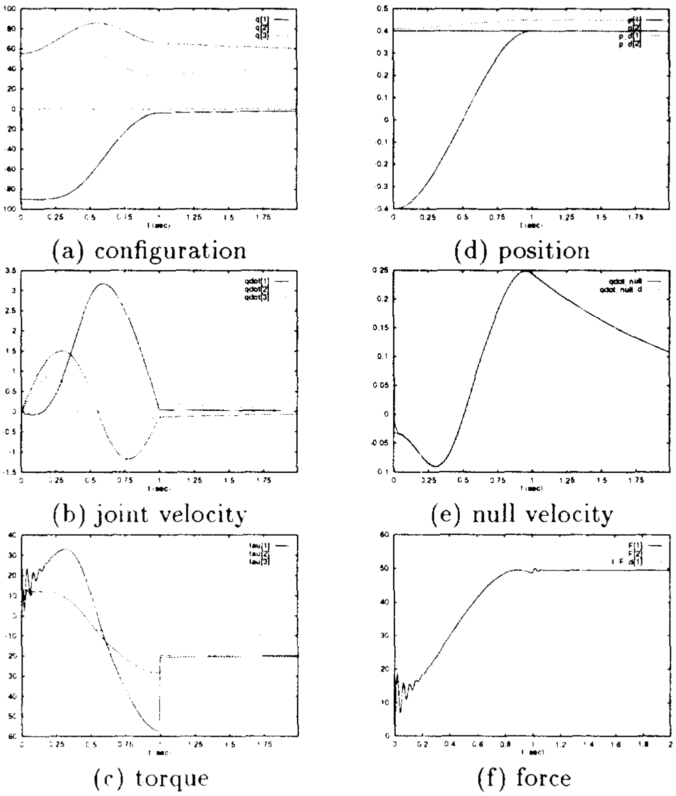

(a) configuration (d) position (b) joint velocity (e) null velocity (c) torque (f) force

Figure 4. Simulation result in impedance control fashion